Available online at www.sciencedirect.com
SCIENCE DIRECT
Polymer 46 (2005) 9686–9693
polymer
www.elsevier.com/locate/polymer

Geometrical influence of AB_n monomer structure on the thermal properties of linear-hyperbranched ether–ketone copolymers prepared via an $AB + AB_n$ route

Eric Fossum[a,**], Loon-Seng Tan[b,*]

[a]Department of Chemistry, Wright State University, 3640 Colonel Glenn Hwy, Dayton, OH 45435, USA
[b]Polymer Branch, Materials and Manufacturing Directorate, AFRL/MLBP, Air Force Research Laboratory, Manufacturing Technology Directorate, 2491 Hobson Way, Wright-Patterson Air Force Base, Dayton, OH 45433-7750, USA

Received 5 May 2005; received in revised form 22 July 2005; accepted 5 August 2005
Available online 6 September 2005

Abstract

A series of poly(ether ketone) copolymers were prepared by nucleophilic aromatic polymerization reactions of 4-fluoro-4′-hydroxybenzophenone, **2**, in the presence of varying percentages of AB_n monomers based on a triarylphosphine oxide platform, **1a** (2F), **1b** (4F), and **1c** (6F), where A = OH and B = F. As expected, the crystallinity of the samples decreased with an increasing AB_n content. However, the tetrahedral geometry of the phosphine oxide-based AB_n monomers proved to be much more efficient at lowering the melt temperature of the copolymers than was the corresponding ketone-based AB_n monomer, 3,5-bis(4-fluorophenylbenzoyl)phenol, **4**, that possesses a structure more similar to that of **2**. Polymerization of **2** in the presence of as little as 5 mol% of bis-(3,4,5-trifluorophenyl)-(4-hydroxyphenyl)phosphine oxide, **1c** (6F), afforded a completely amorphous polymer with a glass transition temperature of 168 °C that was soluble in hot NMP and DMSO. The copolymers also exhibited excellent thermoxidative stability with a number of samples displaying 5% weight loss temperatures, in air, well in excess of 500 °C.
Published by Elsevier Ltd.

Keywords: Copolymerization; Poly(ether–ketone); Thermal properties

1. Introduction

Copolymerization has long been utilized as a tool to modify the chemical and physical properties of polymeric systems [1,2]. In recent years, chain growth polymerization techniques have been employed to provide a wide range of materials with differing topological and morphological characteristics. By combining the advances in radical polymerization processes with the relatively new area of self-condensing vinyl polymerization, a number of linear and branched copolymers have been synthesized. For example, Matyjaszewski et al. have prepared hyperbranched polystyrene via atom transfer radical polymerization techniques [3]. Knauss et al. have prepared a series of branched polystyrene samples, via anionic self-condensing vinyl polymerization, in which the length of the linear polystyrene segments was strictly controlled [4,5].

On the other hand, copolymerization has also been widely used with polycondensation reactions to manipulate or enhance the physical properties and improve the processibility of the final polymer. Of particular interest for the current discussion is the copolymerization behavior of AB and AB_n monomers, as originally described by Flory [6]. A number of authors have utilized this approach to tune the physical properties of copolymers including Kricheldorf et al. for poly(esters) [7–9], Moore et al. for poly(ether-imide)s [10,11], Tan et al. for poly(ether ketone)s [12], and Baek for poly(phenyl quinoxaline)s [13]. Frey has also reported on the copolymerization of AB and AB_n-type monomers, via a slow monomer addition technique, leading to highly branched polyesters and polyglycerols [14–17].

We have been interested in the preparation of highly branched poly(arylene ether) systems based on a

* Corresponding authors. Tel.: +1 937 255 9141; fax: +1 937 255 9158.
** Tel.: +1 937 775 2047; fax: +1 937 775 2717.
E-mail addresses: eric.fossum@wright.edu (E. Fossum), loon-seng.tan@wpafb.af.mil (L.-S. Tan).

0032-3861/$ - see front matter Published by Elsevier Ltd.
doi:10.1016/j.polymer.2005.08.020

triarylphosphine oxide (TPO) platform. Polymerization reactions of **1a** (2F), **1b** (4F), and **1c** (6F), under typical nucleophilic aromatic substitution conditions, provided hyperbranched poly(arylene ether phosphine oxide)s, HB-PAEPO, with number average molecular weights ranging from 10,000 to 15,000 dalton [18].

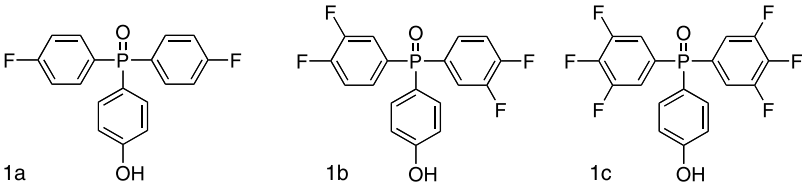

This report describes our efforts to prepare branched (ether–ketone) copolymers, PEK, via copolymerization reactions of 4-fluoro-4′hydroxybenzophenone, **2**, with **1a**, **1b**, and **1c**. The use of **1a**, **1b**, and **1c** provides a versatile system for studying a number of key aspects of AB/AB$_n$ type polymerization reactions including: (1) the effect of monomer reactivity and fluorine content on the thermal properties of the final copolymers, (2) the effect of incorporating an AB$_n$ monomer with a tetrahedral geometry on the crystallinity of the PEK, (3) the degree of branching of the copolymers, and (4) the effect of monomer reactivity on the mode of AB$_n$ monomer incorporation. In addition, the use of the triarylphosphine oxide-based systems as the comonomers should improve the thermal stability of the systems when compared to TPO-free ether–ketone copolymers [12]. The branched structures also provide an opportunity for modification of the end groups to further manipulate the physical and chemical properties of the polymers.

2. Experimental

2.1. Materials

All reactions were performed under a nitrogen atmosphere and all transfers were done using syringes or cannula as necessary. 4-Fluoro-4′-hydroxybenzophenone was purchased from Aldrich Chemical Co. and recrystallized from ethanol prior to use. Potassium carbonate, K_2CO_3, was dried in an oven at 120 °C. Toluene was dried over and distilled from sodium/benzophenone prior to use. *N*-methylpyrrolidinone (NMP), was dried over CaH_2 and distilled prior to use. Monomers **1a** (2F), **1b** (4F), and **1c** (6F) were prepared according to literature procedures [18].

2.2. Instrumentation

^{1}H and ^{31}P NMR spectra were obtained using a Bruker AVANCE DMX 300 MHz instrument operating at 300 and 121.5 MHz, respectively. Samples were dissolved in $CDCl_3$ or DMSO-d_6 as required. Size exclusion chromatography (SEC) analyses were performed using a Viscotek Model 300 TDA system equipped with refractive index, viscosity, and light scattering detectors operating at 70 °C. Polymer Laboratories 5 μm PL gel columns (guard column and two mixed D columns) were used with NMP (with 0.5% LiBr) as the eluent and a Thermoseparation Model P1000 pump operating at 0.8 mL/min. Differential scanning calorimetry (DSC) was performed in nitrogen with a heating rate of 10 °C/min using a Perkin–Elmer DSC 7 thermal analyzer. Thermogravimetric analysis (TGA) was conducted in helium (He) and air atmospheres (gas flow rate of 50 mL/min.) with a heating rate of 10 °C/min using a TA Instruments Hi-Res TGA 2950 thermogravimetric analyzer.

The AM1 semi-empirical method, available as part of the HyperChem Release 7 molecular modeling package [19], was used to optimize the molecular structures of **1a**, **1b**, **1c** and **4**. The following computation set-up was used: total charge = 0, spin multiplicity = 1, lowest electronic (singlet) state; convergence limit = 0.001 kcal/mol; restricted Hartree–Fock (RHF) method for calculating spin interactions, and Polak–Riebiere optimization algorithm was used with RMS gradient set at 10^{-5} kcal/(Å mol). The calculated bond lengths and angles were compared with known experimental values in order to have reasonable confidence in the results. Some selected bond length comparisons are as follows: (i) P=O (experimental value ~1.45 Å as in PO_4^{3-} vs. 1.4740, 1.4726, 1,4712 Å for **1a**, **1b** and **1c** in that order); (ii) C–F (aromatic, experimental value 1.328 ± 0.005 Å vs. 1.3521 and 1.3521 Å for **1a**; 1.3519 and 1.3528 Å (meta to phosphorus)), 1.3494 and 1.3494 Å (para to phosphorus) for **1b**; 1.3509, 1.3518, 1.3509, and 1.3518 Å (meta to phosphorus) and 1.3470, 1.3470 Å (para to phosphorus) for **1c**; (iii) C–O (phenol, experimental value 1.36 ± 0.01 Å), 1.3709, 1,3694, 1.3691 and 1.3781 Å for **1a**, **1b**, **1c** and **4**.

2.3. Typical procedure for the copolymerization of *2* with *1a–c*

In an oven dried 100 mL round-bottom flask equipped with a magnetic stir bar, Dean Stark trap, and nitrogen inlet were placed 1.50 g (6.91 mmol) of **2**, 0.77 g (2.34 mmol) of **1a** (1F), 1.60 g (11.57 mmol) of potassium carbonate, 20.0 mL of freshly distilled NMP, and 20.0 mL of dry toluene. The flask was immersed in an oil bath and the temperature was raised to 160 °C and held there for 4 h to complete the azeotropic drying process. After 4 h the

toluene was removed by slowly increasing the temperature to 202 °C. The vigorously stirred mixture was kept at 202 °C until the viscosity became too high for the stir bar to work effectively at which point the solution was diluted with NMP (20 mL) and slowly poured into 500 mL of rapidly stirred distilled water to afford an orange/peach colored solid that was isolated by filtration. The solid was transferred to an extraction thimble and extracted with water, followed by methanol for 24 h each. The off-white solid was subsequently dried in a drying pistol at 115 °C for 8 h before analysis. The reaction progress was monitored by removal of small aliquots at various intervals for analysis via SEC and ^{31}P NMR spectroscopy.

3. Results and discussion

3.1. Monomer geometry

The structures of the AB_n monomers, **1a** (2F), **1b** (4F), **1c** (6F), and **4** (2F), where the number of potentially chemically labile fluoride atoms are indicated in the parentheses, were optimized using the semi-empirical AM1 computation program (Hyperchem ver. 7, Hypercube, Inc.) and are shown in Fig. 1. Monomers **1a** and **4** have similar molecular weights, 329 g/mol for **1a** and 338 g/mol for **4**, but the reactivity of the electrophilic sites should be significantly different. In addition, while **1a** (1F) cannot adopt a planar geometry without severe distortions of the structure, a planar geometry is easily envisioned for **4**. This is indeed the case in comparing their computationally optimized structures (Fig. 1). Therefore, it was anticipated that the tetrahedral geometry of **1a** would provide a more efficient disruption of the chain packing of the linear PEK segments than would **4**. Similar effects would be anticipated for **1b** and **1c** as well.

3.2. Polymerization

Branched copoly(ether ketone)s incorporating the triarylphosphine oxide group were prepared according to the route shown in Scheme 1. Initial copolymerization experiments were performed with 25 mol% of **1a** (2F), **1b** (4F), and **1c** (6F), respectively, and the molecular weight results are listed in Table 1. The reaction mixtures were azeotropically dried for 4 h at which point the toluene was removed and the reaction temperature was increased to 202 °C. Immediate differences in the behavior of **1a**, **1b**, and **1c** in the copolymerization reactions were observed. For example, with **1a** the reaction mixture became very difficult to stir after 1 h, with **1b** the same point was reached at two hours, whereas with **1c** the solution did not reach such a high viscosity even after 2 h at 202 °C. Ostensibly, the observed polymerization behavior translated directly to the resulting solubility characteristics of the systems.

After the work-up that involved precipitating the polymers from water followed by Soxhlet extractions with methanol and water, the resulting off-white polymers possessed very different solubility characteristics (Table 1). Interestingly, while the copolymers from **1b** (4F) and **1c** (6F) were soluble in room temperature NMP, DMSO, and DMAc, the (25/75) copolymer prepared from **1a** (2F) required the use of hot NMP, DMSO, or DMAc for dissolution. Upon cooling the copolymer from **1a** remained soluble in NMP thus allowing for analysis of all three (25/75) copolymers by size exclusion chromatography (SEC). Subsequent reactions were performed with 5–10 mol% of **1a** and **1b**, and 3–10 mol% of **1c** as the co-monomer for **2**. As the percentage of AB_n monomer was decreased, the

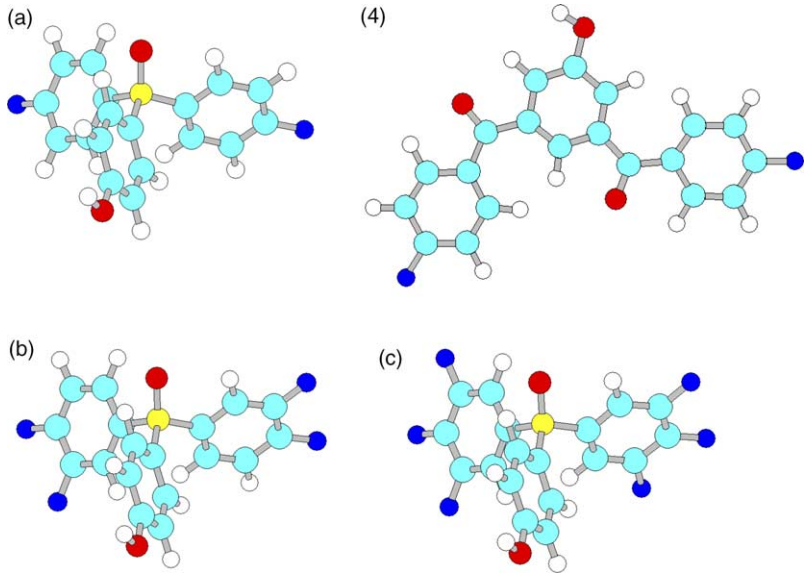

Fig. 1. AM1 optimized structures for **1a** (2F), **1b** (4F), **1c** (6F), and **4**.

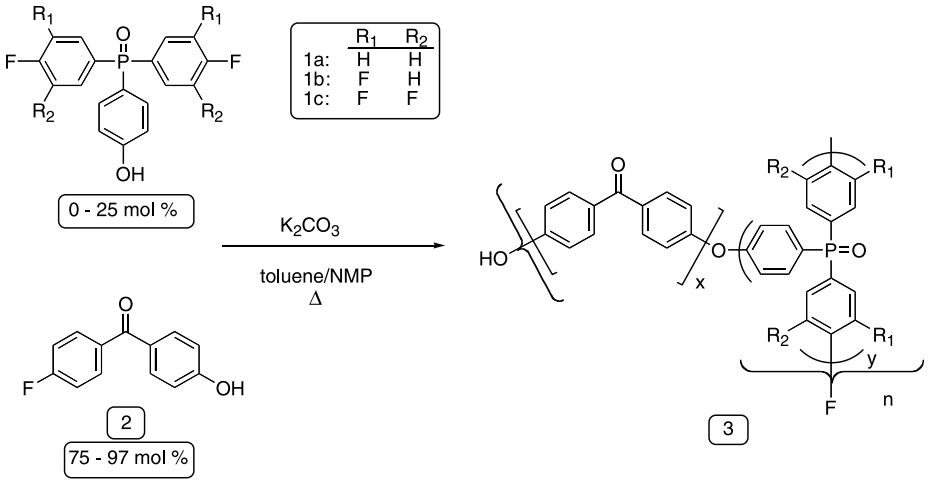

Scheme 1.

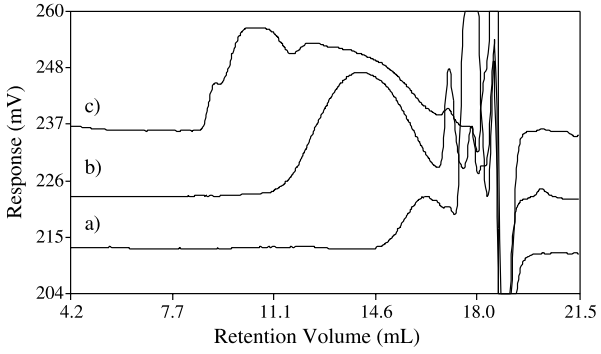

Fig. 2. SEC traces (RI detector) of samples taken from the reaction of 25 mol% of **1a** and 75 mol% of **2**: (a) just after toluene removal, (b) 20 min after toluene removal, and (c) 40 min after toluene removal.

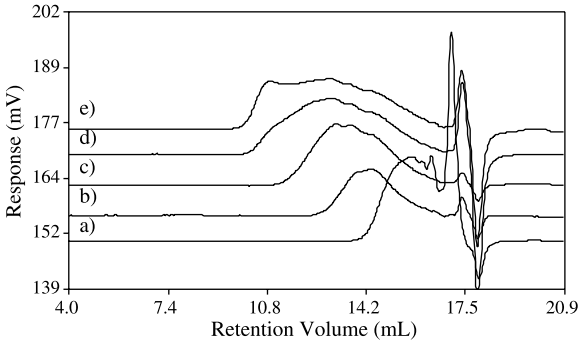

Fig. 3. SEC traces (RI detector) of samples taken from the reaction of 25 mol% of **1b** and 75 mol% of **2**: (a) just before toluene removal, (b) just after toluene removal, (c) 30 min after toluene removal, (d) 60 min after toluene removal, and (e) 100 min after toluene removal.

Table 1
Molecular weight and solubility data for linear poly(arylene ether ketone)-*co*-hyperbranched poly(arylene ether phosphine oxide) copolymers, PEK/HB PAEPO

mol% **1a–c**	mol% **2**	NMP	DMAc	DMSO	M_n (dalton)	M_w (dalton)	PDI
1a	**2**						
100	0	++	++	++	12,400	33,360	2.69
25	75	+−	+−	+−	13,000	143,000	11.0
10	90	−	−	−	- - -	- - -	- - -
5	95	−	−	−	- - -	- - -	- - -
1b	**2**						
100	0	++	++	++	14,600	52,560	3.60
25	75	++	++	++	12,500	218,750	17.5
10	90	+−[a]	−	+−[a]	- - -	- - -	- - -
5	95	−	−	−	- - -	- - -	- - -
1c	**2**						
100	0	++	++	++	9200	22,450	2.44
25	75	++	++	++	6250	10,000	1.60
10	90	++	++	++	6520	20,400	3.13
5	95	+−[a]	+−[a]	+−[a]	- - -	- - -	- - -
3	97	+−[a]	−	+−[a]	- - -	- - -	- - -

++, Represents solubility at room temperature (1–3 mg/mL at rt); +−, represents solubility when heated (1–3 mg/mL at 150 °C); −, represents insoluble (1–3 mg/mL at 150 °C).

[a] Unlike the (25/75) copolymer of **1a** with **2**, these copolymers did not sustain the complete dissolution upon cooling down to room temperature, precluding reliable SEC determination.

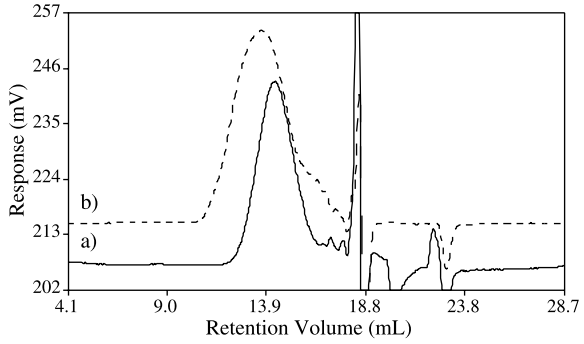

Fig. 4. SEC traces (RI detector) of samples taken from the reaction of (a) 25 mol% of **1c** and 75 mol% of **2** and (b) 10 mol% of **1c** and 90 mol% of **2**, both after 2 h of reaction time after toluene removal.

solubility of the copolymers decreased as well, which was not surprising given the fact that PEK itself is highly crystalline and extremely insoluble.

3.3. Molecular weights

The number average and weight average molecular weights, M_n and M_w, respectively, of the samples that remained soluble in NMP at room temperature were determined via SEC (Figs. 2–4) and the results are listed in Table 1. For comparison purposes, the M_n and polydispersity index, PDI, values of the homopolymers prepared from **1a**, **1b**, and **1c** are included. With the exception of **1c**, the M_n values are comparable to those of the homopolymers. However, the PDI values for the copolymer samples are much higher than those for the homopolymer samples. For example, with **1b**, the copolymer at a ratio of 25:75 (**1b**:**2**) had a PDI value of 17.5 while that for the homopolymer of **1b** was only 3.60. This dramatic difference can be explained if intramolecular cyclization is considered. The homopolymer of **1b** most likely possesses a significant presence of polymer molecules that have undergone intramolecular cyclization. When a significant quantity of **2** is present in the system, its more rigid and planar structure has the potential to limit the intramolecular cyclization process. The absence or retarding of intramolecular cyclization would lead to a significant increase in the observed PDI value [20–23]. Unfortunately, as the mole percentage of **1a**, **1b**, and **1c** was decreased, the polymer samples could no longer be analyzed via SEC as they did not remain soluble in NMP after cooling to room temperature.

The AB_n monomers with higher fluorine contents tended to provide copolymers with better solubility properties. This observation may be attributed to the fluorine content itself, but may also be a result of the actual number of functional groups present in **1a** (2F), **1b** (4F), and **1c** (6F). While **1a**, **1b**, and **1c**, are considered to be AB_2 monomers, the actual number of electrophilic sites in **1b** and **1c** may approach 4 and 6, respectively. We have observed multiple substitutions on the same phenyl rings when *tris*-(3,4-difluorophenyl)phosphine oxide and *tris*-(3,4,5-trifluorophenyl) phosphine oxide were reacted under similar conditions [24].

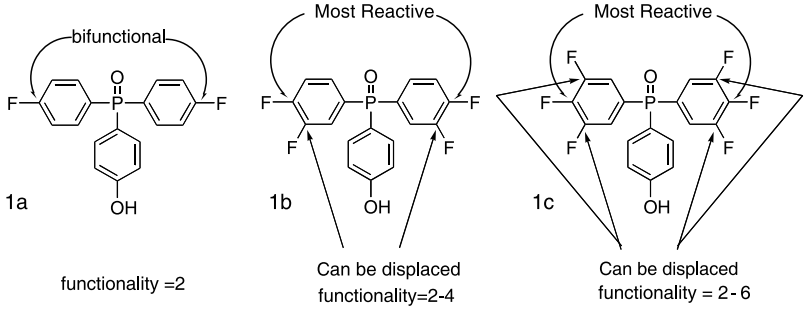

If **1b** and **1c** were to undergo multiple nucleophilic aromatic substitution reactions on the same ring, the resulting polymers would be highly branched leading to the enhanced solubility. This may also help to explain the relatively low PDI values observed for the copolymers prepared with **1c**. The increased branching structure would enhance the ability of the polymers to react through an intramolecular cyclization process resulting in lower PDI values as well as limited molecular weights. One other plausible explanation for the observation of a decrease in PDI values with **1c** might be a narrowing in the average hydrodynamic volume because of repulsion among the fluorine atoms at the surface.

These effects can be clearly seen in Figs. 2–4, corresponding to the 25 mol% copolymers of **1a**, **1b**, and **1c**, respectively. In Fig. 2 (25 mol% **1b**), the weight-average molecular weight (M_w) of the polymer continues to grow,

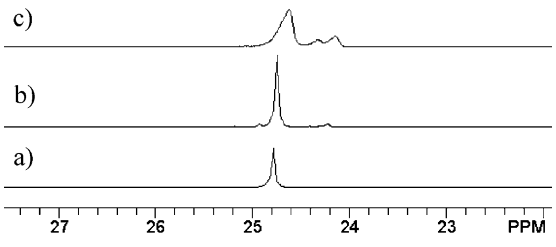

Fig. 5. ^{31}P NMR spectra (DMSO-d_6) of samples taken from the reaction of 25 mol% of **1a** with 75 mol% of **2**: (a) **1a**, (b) sample just before toluene removal, and (c) sample taken just after toluene removal.

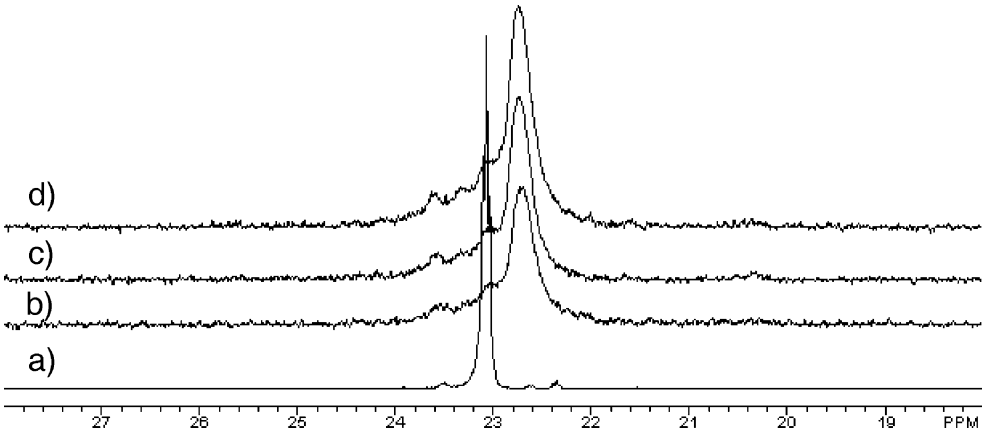

Fig. 6. ^{31}P NMR spectra (DMSO-d_6) of samples taken from the reaction of 25 mol% of **1b** with 75 mol% of **2**: (a) **1b**, (b) sample 1 h after toluene removal, (c) sample taken 1.5 h after toluene removal, and (d) sample taken 2 h after toluene removal.

and the PDI continues to broaden as the reaction progresses. Similar observations are observed in Fig. 3 (25 mol% **1b**). Fig. 4 displays the SEC traces of the final products from copolymerization reactions of 25 and 10 mol% of **1c**. Both traces display a much lower M_w and lower PDI than the traces from reactions with 25 mol% of **1a** or **1b**. In addition, the M_w and PDI of the copolymer prepared with 10 mol% of **1c** is significantly higher than that of the sample prepared with 25 mol% of **1c** lending credence to the above arguments for the presence of intramolecular cyclization.

3.4. Incorporation of AB_n component via ^{31}P NMR spectroscopy

The final sample of the copolymer with 25 mol% of **1a** (2F) was not soluble in DMSO-d_6 whereas both copolymers from **1b** (4F) and **1c** (6F) were completely soluble in the same solvent and allowed for analysis using ^{31}P NMR spectroscopy. However, samples of the reaction with **1a** taken before the reaction reached completion were completely soluble in DMSO-d_6. The ^{31}P NMR spectra (Figs. 5–7) of the polymer samples provided an indication how the AB_n components were incorporated.

Fig. 5 depicts the ^{31}P NMR spectra of the first two samples taken from the copolymerization reaction with 25 mol% of **1a** (2F) and indicated, that at least initially, **1a** is incorporated in two different modes, most likely as a linear component and a dendritic unit. Unfortunately, the polymers become insoluble at higher M_w's and the corresponding ^{31}P NMR spectra were not acquired.

Fig. 6 depicts the ^{31}P NMR spectra of the samples taken from the copolymerization reaction with 25 mol% of **1b** (4F). It is apparent that the majority of **1b** is incorporated into the copolymer via one mode, presumably as dendritic components, and the spectra do not change considerably with reaction time. The small downfield signals appear to increase in intensity with reaction time and these might correspond to signals from polymers that have undergone intramolecular cyclization.

Fig. 7 depicts the ^{31}P NMR spectra of the samples taken from the copolymerization reaction with 25 mol% of **1c** (6F). The spectra indicate that a majority the **1c** component is incorporated into the copolymer at a very early stage, just after the toluene removal. The spectra show only slight variations over time with only a small downfield signal increasing slowly with time, as well as a two minor upfield

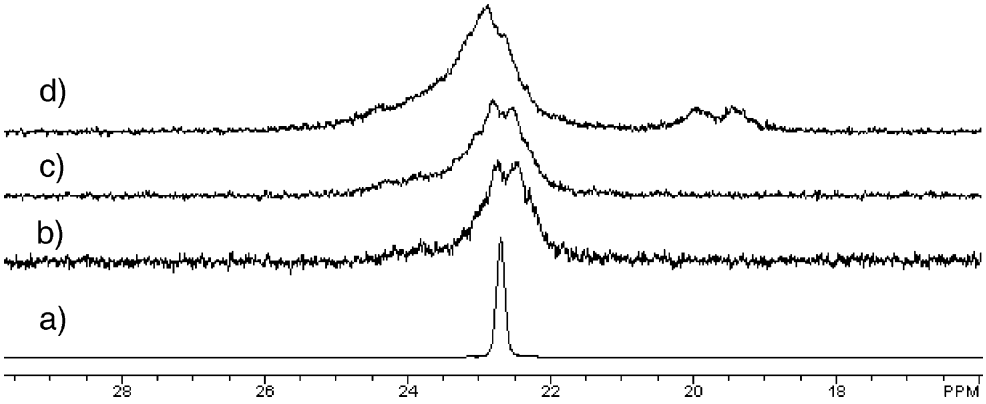

Fig. 7. ^{31}P NMR spectra (DMSO-d_6) of samples taken from the reaction of 25 mol% of **1c** with 75 mol% of **2**: (a) **1c**, (b) sample just after toluene removal, (c) sample taken 30 min after toluene removal, and (d) final sample taken 2 h after toluene removal.

signals present in the final spectrum. These subtle changes indicate that the reaction of **1c** is essentially complete at an early stage and subsequent grow occurs primarily with the AB component.

3.5. Thermal analysis

3.5.1. Differential scanning calorimetry

All of the polymer samples were analyzed via DSC to determine their glass transition temperatures, T_g, and melting temperatures, T_m. With the exception of the copolymers prepared with **1c** (6F), there was a continuous decrease in the T_g values as the percentage of AB_n monomer was decreased. For example, with 25 and 5 mol% of **1a** (2F), the T_g values were 184 and 167 °C, respectively. With **1b** (4F), the effect was even more dramatic as 25 and 5 mol% of **1b** led to T_g values of 201 and 161 °C, respectively. The larger decrease in T_g values with **1b** vs. **1a** may be a direct result of the increased branching that is possible with **1b**. The more highly branched structures that are possible with **1b** should have more hindered motions resulting in higher T_g values being observed. Also, analogous to poly(vinyl fluoride), $T_g = 64$ °C, and poly (vinylidene fluoride), $T_g = -35$ °C [25], an increase in the fluorine content from **1a** to **1b** may also be responsible for the decrease in T_g from **1a** to **1b**.

With **1c** (6F) the exact opposite trend is observed and at a first glance this observation might be counterintuitive if the thermal analysis data is looked at exclusively. However, when the data are analyzed in conjunction with the molecular weight data a clearer picture emerges. The increased T_g values observed as the mol% of **1c** is decreased may simply be a result of the formation of higher molecular weight materials. As the mol% of **1c** is decreased, the tendency to undergo intramolecular cyclization reaction should also decrease and the polymerization should become more like a 'normal' hyperbranched polymerization in which the M_w and PDI values increase dramatically near the end stages of the reaction. The presence of much higher M_w materials would lead to the observed increase in T_g values.

The influence of the tetrahedral geometry on the ability of the copolymers to crystallize is readily apparent by the absence of a T_m value for most of the samples prepared in this study. The only two samples that possess any observable T_m values are at 5 mol% of **1a** and **1b** with T_m values of 331 and 316 °C, respectively. These results indicate that the tetrahedral geometry is highly efficient at hindering crystallization in these systems. It is interesting to note that even the sample with only 3 mol% of **1c** did not possess a T_m giving further evidence for the actual number of electrophilic sites present in **1b** and **1c**.

3.5.2. Thermogravimetric analysis

It is well established that incorporating the triarylphosphine oxide moiety into linear polymers gives rise to a considerable increase in the thermal stability of the material [26,27]. Since comparable thermal stability was also reported for TPO-containing hyperbranched polymers [18,28,29], similar stability is expected for the copolymers currently under study. Thus, all of the samples in this study were subjected to analysis via TGA, both under helium and air. The 5% weight loss temperatures in air decreased consistently with a decreased mol% of **1a** with values of 521, 516, and 490 °C being determined for 25, 10, and 5 mol% of **1a**, respectively. A similar trend was observed in a helium atmosphere. The trend was not so clear with **1b** and

Table 2
Thermal property data for linear poly(arylene ether ketone)-*co*-hyperbranched poly(arylene ether phosphine oxide) copolymers, PEK/HB PAEPO

mol% **1a–c**; **4**	mol% **2**	T_g (°C)	T_m (°C)	T_d (°C) 5% In air	T_d (°C) 5% In helium
1a					
100	0	234	–	533	560
25	75	184	–	521	550
10	90	175	–	516	549
5	95	167	331	490	530
1b					
100	0	232	–	393	363
25	75	201	–	522	535
10	90	181	–	500	562
5	95	161	316	527	567
1c					
100	0	220	–	347	352
25	75	147	–	420	435
10	90	144	–	470	520
5	95	168	–	470	485
3	97	172	–	505	552
4					
39.1[a]	60.9	210.3	–	411	432
17.5[a]	82.5	170.0	339.5	426	462
0[a]	100	174.6	360.5	461	463

[a] Data taken from Ref. [12].

1c as the 5% weight loss temperatures fluctuated considerably across the sample range. However, it can be stated that all the samples prepared in this study did possess considerably higher 5% weight loss temperatures than PEK itself and the copolymers prepared with **4** (Table 2). Finally, in comparing the 5% weight loss temperature data for the parent hyperbranched polymers of **1b** and **1c**, rather surprising was the trend that both the thermal (helium) and thermo-oxidative stability (air) data decreased with an increase in the terminal fluoride groups [30]. This is in contrast to the general observation that fluorinated polymers are higher in thermal and thermo-oxidative stability than their non-fluorinated analogues (e.g. 6F-bisphenol A-based polymers vs. bisphenol A analogues).

4. Conclusions

A series of poly(ether ketone)-based copolymers were prepared by polymerization reactions of mixtures of **2** with **1a** (2F), **1b** (4F), or **1c** (6F) in molar ratios of 75:25, 90:10, 95:5, and 97:3 (**1c** only). The incorporation of the tetrahedral AB_n comonomers increased the solubility of the resulting materials, relative to linear PEK, while decreasing the ability of the PEK segments to crystallize. The more rigid AB monomer, **2**, tended to limit any intramolecular cylization processes with the result being considerably higher PDI values for the current samples when compared to the homopolymers of **1a**, **1b**, or **1c**. The crystallinity of the PEK segments was completely suppressed when greater than 5 mol% of **1a** or **1b** was utilized as the comonomer whereas as little as 3 mol% of **1c** was sufficient to prevent any crystallization. All of the samples exhibited excellent thermal stability characteristics with copolymers of **1a** possessing 5% weight loss temperatures in excess of 500 °C when 10 or more mol% of **1a** was utilized. Ongoing work involves the determination of the relative reactivity ratios of the AB and AB_n monomers.

Acknowledgements

The authors wish to thank Marlene Houtz for performing the thermal analysis measurements. E.F. wishes to thank the Air Force Office of Scientific Research for supporting work on this project through the Air Force Research Laboratory-Summer Faculty Fellowship Program.

References

[1] Platzer NAJ. In: Platzer NAJ, editor. Copolymers, polyblends, and composites. Advances in chemistry series, vol. 142. Washington, DC: American Chemical Society; 1975.
[2] Odian G. Principles of polymerization. 3rd ed. Hoboken, New Jersey, USA: Wiley; 2004. p. 135–143.
[3] Gaynor SG, Edelman S, Matyjaszewski K. Macromolecules 1996;29:1079.
[4] Knauss DM, Al-Muallem HA, Huang T, Wu DT. Macromolecules 2000;33:3557.
[5] Al-Muallem HA, Knauss DM. J Polym Sci, Part A: Polym Chem 2001;39:152.
[6] Flory PJ. J Am Chem Soc 1952;74:2718.
[7] Kricheldorf HR, Lohden G. J Macromol Sci, Pure Appl Chem 1995;A32:1915.
[8] Kricheldorf HR, Stober OS, Lubbers D. Macromol Chem Phys 1995;196:3549.
[9] Kricheldorf HR, Stukenbrock T. Polymer 1997;38:3373.
[10] Markoski LJ, Moore JS, Sendijarevic I, McHugh AJ. Macromolecules 2001;34:2695.
[11] Markoski LJ, Thompson JL, Moore JS. Macromolecules 2000;33:5315.
[12] Baek J-B, Tan L-S. Polymer 2003;44:3451.
[13] Baek J-B, Harris FW. Macromolecules 2005;38:1131.
[14] Hanselmann R, Holter D, Frey H. Macromolecules 1998;31:3790.
[15] Mock A, Burgath A, Hanselmann R, Frey H. Macromolecules 2001;34:7692.
[16] Kautz H, Barriau E, Chen Y, Collado MP, Wissert R, Frey H. Polym Mater Sci Eng 2003;88:549.
[17] Burgath A, Mock A, Hanselmann R, Frey H. Polym Mater Sci Eng 1999;80:126.
[18] Bernal DP, Bankey NB, Cockayne RC, Fossum E. J Polym Sci, Part A: Polym Chem 2002;40:1456.
[19] HyperChem Version 7.5, www.hyper.com.
[20] Burgath A, Sunder A, Frey H. Macromol Chem Phys 2000;201:782.
[21] Chu F, Hawker CJ, Pomery PJ, Hill DJT. J Polym Sci, Part A: Polym Chem 1997;35:1627.
[22] Komber H, Ziemer A, Voit B. Macromolecules 2002;35:3514.
[23] Kricheldorf HR, Schwarz G. Macromol Rapid Commun 2003;24:359.
[24] Bedrossian L, Fossum E. ACS Div Polym Chem, Polym Prepr 2004;45:1049.
[25] Mark JE, editor. Polymer data handbook. New York: Oxford University Press; 1999. p. 942–51.
[26] Smith Jr JG, Connell JW, Hergenrother PM. Polymer 1994;35:2834.
[27] Smith CD, Gungor A, Wood PA, Liptak SC, Grubbs H, Yoon TH, et al. Macromol Chem, Macromol Symp 1993;74:185.
[28] Lin Q, Long TE. J Polym Sci, Part A: Polym Chem 2000;38:3736.
[29] Lee HS, Takeuchi M, Kakimoto M-a, Kim SY. Polym Bull 2000;45:319.
[30] A reviewer suggested that the early weight loss of hyperbranched polymers from **1b** and **1c** compared to **1a** might originate from a higher population of low molecular weight species resulting from intramolecular cyclization.